DOI: 10.13009/EUCASS2019-786

DOI: ADD DOINUMBER HERE

Plasma flow control in a rarefied Mach 20 Flow over a flat plate

Viviana Lago[⋆†], *Romain Joussot and Sandra Coumar* [⋆]
[⋆]*CNRS, ICARE, UPR 3021*
1c av. de la Recherche Scientifique, CS 50060, F-45071, Orléans Cedex 2, France.
viviana.lago@cnrs-orleans.fr · sandra.coumar@cnrs-orleans.fr · romain.joussot@cnrs-orleans.fr
[†]viviana.lago@cnrs-orleans.fr

Abstract

This paper presents an experimental investigation focusing on plasma flow control efficiency in hypersonic and rarefied regime. This work was carried out at the ICARE laboratory by the Fast team with the hypersonic an rarefied facility MARHY (ex SR3). Experiments concern the modification of the flow field above a sharp flat plate using a surface plasma actuator. The working condition is defined by a Mach 20.2 flow, with a static pressure of 0.068 *Pa* simulting pressure conditions at 100*km* of altitude. The plasma actuator is an aluminium alectrode placed at the leading edge of the plate and biased with a nanosecond pulsed power supply. A range of repetition rate pulse and output voltages values have been invetigated to evluate their efficiency. Flow field modifications were observed with an iCCD intensified camera and the analysis of the images showed the modification of the shock wave shape and the angle increase for all experimental conditions.

1. Introduction

At the beginning of 50s, when the space flight was becoming reality, atmospheric re-entry problems were not thought as difficult or even dangerous. Enthusiastic and bold previsions were made for space missions until the first experimentations, where it was quickly seen that this will not be as easy as expected.

During atmospheric re-entries, space vehicles reach hypersonic speeds that can reach Mach 40 because of the action of the gravity force which attracts the entering object strongly toward the planet whereas the vacuum state of the space puts up no resistance to its movement. Some planets are surrounded by an atmosphere, that at the high speeds reached by the space vehicles, the atmosphere appears as a dense and thus, dangerous medium. A re-entry mission relies on the good management of the entry angle and speed, which have to be as precise as possible to ensure an efficient landing.[13] The gravitational as well as the aerodynamic forces increase on the object as the altitude decreases and usually becomes dominant by 40 *km* as a result of the exponential increase of the air density.[7] Thus, even with optimal entry parameters, when passing through the dense layers of the atmosphere, the space vehicle rubs powerfully with surrounding air molecules inducing great friction and heat load on its structure.

An easy calculation allows us to understand one of the main issue ensured by the re-entry vehicle, i.e the accumulated heat load on its surface. The kinetic energy equation per unit mass is: $E = \frac{1}{2}V_o^2$, where V_o is the orbital velocity. Let consider an initial entry speed of 11 $km.s^{-1}$ which is usual for man-built vehicles and a final velocity very small, reduced to $V_o = 0.5\ km.s^{-1}$ for landing. This leads to a decrease of 95.5% in the speed and 99.8% in the kinetic energy per unit mass. This energy, concentrated in the spacecraft is dissipated during the entry phase that lasts mostly in the range of the minutes, for instance, 5 minutes. That means that a total kinetic energy of 60.4 $MJ.kg^{-1}$ has to be dissipated in 5 minutes.

Therefore, the complexity of the atmospheric entries is the thermochemical non-equilibrium due the very high-speeds. Indeed, the characteristic time of the flow becomes very small and in the range of the times of the physico-chemical phenomena. This shows that atmospheric entries are different to the combustion domain where the temperatures are weaker and there is no thermal disequilibrium, and even different from the cold plasmas where the electrons role is more important or the domain of the fusion where the species are strongly ionized. The physico-chemical of high-enthalpy gas are still little known and is mostly answered by introducing bigger security margins than needed for the thermal protections. However, if planning longer distances missions, it is vital to restrict these margins as possible and thus, predict in a more efficient way the encountered phenomena. Most of the uncertainties concern:

DOI: 10.13009/EUCASS2019-786

- chemical kinetics of the neural and ionized species at high temperatures
- electronic properties (energy distribution function, plasma density) linked to the plasma frequency and happening in the radio-frequency disturbances (black-out)
- excitation phenomena of the internal modes and couplings
- radiative process.

Since then, the struggle remains and nowadays the best solution to this problem stays the Thermal Protection System (TPS) which acts like a shield around the vehicle. In order to avoid complete destruction of the vehicle, a thermal protection system (TPS) is built upfront the vehicle and burns heavily.

The TPS technology is strongly studied and three variations can be highlighted: hard TPS, deployable TPS and new shapes. The hard ones are the usual TPS that are fixed on the structure of the vehicle but advances are required to significantly lower the mass of the TPS and even if new tailored materials like woven instead of carbon are planned, improvements can still be made. The deployable shields would be lighter because they would be inflated or deployed only for the re-entry process but entail issues like the TPS development complexity, system scalability, aerodynamic shape stability, and areal mass so are still challenging. The third idea relates on changing the aeroshell shapes that have not been modified since the Apollo project. As one can easily imagine, this is essential for new missions but as it consists in a new challenging project that will take time, cost a lot and is for the moment in a conceptual stage. Therefore, even if the TPS is a major technique in atmospheric entry process, it should not and can not be the only one.

The mission planning for re-entry process must delicately balance three requirements: deceleration, heating management and accuracy of the localization and velocity when landing. Indeed, these requirements of re-entry missions strongly depend on the drag force which is the dominant force over all others, including gravity and lift. The drag force plays a key role because it influences deceleration, having then a beneficial direct effect on heat loads, vehicle designs and re-entry trajectory. Therefore, coupled with the TPS, decelerators would be a nice way to ensure a good landing. Many Entry Descent Landing (EDL) techniques are under prospect as attached deployable decelerators, parachutes, retro propulsion or improved Guidance Navigation Control (GNC), and in this purpose, this works focus on a new method based on plasma actuation. Indeed, it has been demonstrated that plasma actuators offer the possibility to modify the shock wave shape around the vehicle and thus, the drag coefficient. This could also potentially reduce the local heat flux and to this regard, plasma-based devices appear as one of the promising technologies to act on drag force.

Compared to traditional flow control methods, plasma actuators present several advantages like their fast response time, their low weight and size and the relatively low energy consumption, offering promising applications for flight control systems at high velocities. Moreover, plasma actuators could help to avoid black-out transmission when being coupled to Magneto-Hydrodynamics (MHD) to optimize communication links.

Although many works deal with plasma control applied to supersonic flow, only few concern rarefied flows. Shin *et al.*,[18] have investigated such kind of flow but without clear evidence of plasma actuation even if they observed two distinct discharge modes. Surzhikov *et al.*[19] have done a very interesting work on the discharge modelling in rarefied regime with external magnetic field conditions but their study is only focused on the discharge modelling without analysing the interaction with a flow. Palm *et al.*,[16] have clearly demonstrated some plasma actuation in a rarefied supersonic flow with a model configuration similar to the cylinder model studied by the FAST team in Lago *et al.*,.[11] Nevertheless, in such case, the boundary layer interaction and the shock wave modification are different to the ones occurring in the present work. Our study relays on hypersonic vehicles that are submitted to great variations of the atmosphere and big changes in pressure, gas density and sound speed depending on the atmospheric altitude thus, introducing effects on lift, drag and pitching moment. These vehicles need to operate in several flight regimes dealing with the optimization of Lift to Drag (L/D) shape during the three phases of an hypersonic fly: climb, cruise flight and landing. The use of plasma actuators could be in the future an alternative to complex geometry design for hypersonic vehicles and atmospheric entry probes for which recent experience have demonstrated that there are still improvements to be done.

The technique using plasma actuators also presents some issues. The main limitation of such actuators is due to the flow conditions, especially the pressure and, thus, the altitude of the atmospheric re-entry of the spacecraft. Plasma actuators have to be characterized in different flow regimes in terms of speed and pressure to extrapolate their behaviour to real cases. For this purpose, it is necessary to deeply understand the plasma physics and its coupling with the flow to overcome these challenges. Therefore, the Fast team of the laboratory ICARE carried out experimental investigations to study the ability of the use of plasma actuators at high Mach number and high altitudes meaning low pressure. Previous study were carried out in the Marhy wind-tunnel of ICARE in which a sharp flat plate equipped with a plasma actuator interacts with a Mach 2 flow at a static pressure of 8 Pa. Experimental studies reported in,[14 15 12] conducted at supersonic and rarefied regime showed that the plasma actuator increases the shock angle. Monte Carlo investigation carried out method showed that this effect is due in part to the surface heating of the flat plate but is not

DOI: 10.13009/EUCASS2019-786

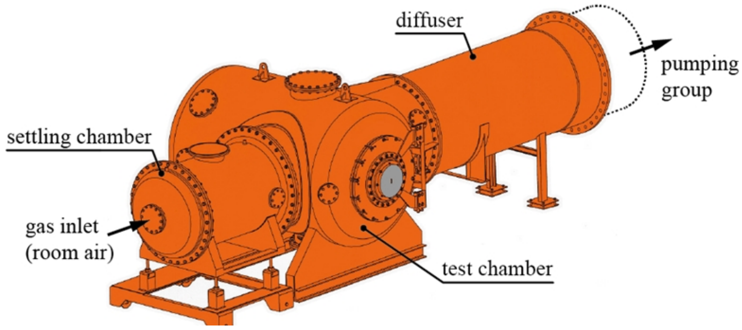

Figure 1: The Marhy wind tunnel lay-out.

due to 'ionic wind' or volume heating. In;[9],[8] experiments were carried out with a heater instead of the plasma actuator, in order to quantify the role of the surface heating showing that it accounts for 50% at most. The other 50% is due to the ionization produced by the plasma discharge created by the plasma actuator which modifies the flow properties and the flow interaction with the flat plate. In[4] and,[5] numerical simulations were carried out with a Navier Stokes code adapted with slip conditions to rarefied regime, to evaluate the drag and lift force. Results showed that a 13% increase in the drag coefficient could be achieved with the plasma actuator in our experimental conditions. In[6] the experimental investigation highlighted how this type of plasma actuator reacts in different flow conditions specially for static pressure condition. Indeed during atmospheric re entry the vehicle will pass through different atmospheric layers with different pressures and Mach numbers, and the topology of a given discharge strongly depends on the ambient pressure, and its interaction with the flow depends on pressure.[10] This work propose a comparative study based on the same model and discharge configuration placed in different flow conditions : Mach 2 / 8 Pa, Mach 4/ 8 Pa and Mach 4/ 71 Pa.Results have shown that in the range of the discharge current applied to the plasma actuator (1 *mA* to 50 *mA*), the shock wave angle increases by 1.15 with the nozzle N1 (M2 - 8 Pa) and by 1.21 and 1.28 with the nozzles N2 (M4 - 8 Pa) and N3 (M4 - 71 Pa) respectively. It was also noticed that the power consumption decreases when increasing the static pressure. This effect is due to the mean free path which decreases with the Mach number and with the pressure.The morphology of the plasma discharge strongly depends on the static pressure. For a static pressure of 8 *Pa*, the plasma is very diffused and extends in the upstream direction while it is confined to the flat plate surface and reattaches to the grounded electrode for the flow at 71 *Pa*. For this condition, the plasma actuator produces a thin layer of plasma over the plate surface producing a bluntness effect on the sharp flat plate.

The present paper presents the results obtained with a Mach 20 flow and a static pressure simulating 100 km in altitude.for this study a pulsed discharge was chosen, rather than a dc as was used for previous hypersonic studies because the pressure level is much lower and this type of discharge improves the ionization level of the gas.[3]

2. Experimental setup

2.1 The MARHy wind-tunnel

The MARHy low density facility of the ICARE laboratory (CNRS, France) is used for both academic and industrial research and can be configured in supersonic and hypersonic running conditions.[1] A schematic view of the facility is presented in Figure 1. It consists of three main parts: the settling chamber with a diameter of 1.3 *m* and a length of 2.0 *m*, the test chamber with a diameter of 2.3 *m* and a length of 5.0 *m*, and a third chamber in which a diffuser is installed. The diffuser is connected to the pumping group by a motor drive butterfly control valve of 1.5 *m* in diameter. A powerful pumping group with 2 primary pumps, 2 intermediary Roots blowers and 12 Roots blowers ensures the low density flow conditions in continuous operating mode. The running configuration of the pumping group, meaning the number of pumps to be used, depends on the experimental flow conditions to be reached. A set of nozzles have been developed and tested to generate subsonic, supersonic and hypersonic flows in low pressure conditions ranging from Mach 0.8 to Mach 21. The obtained experimental running conditions cover a large range of Reynolds numbers from 10^2 up to 10^5 for a reference length of 100 *mm* (corresponding to the length of the flat plate used as model) in rarefied regime.

The present work was carried out with the conical hypersonic nozzle configured to delivers a Mach 20.2 flow with a static pressure of 0.068 *Pa* in the test chamber. The gas used is pure nitrogen and to avoid condensation in the test chamber the gas is heated up to 1100 *K* before the inlet of the throat with a heater based on a graphite resistor. Flow

DOI: 10.13009/EUCASS2019-786

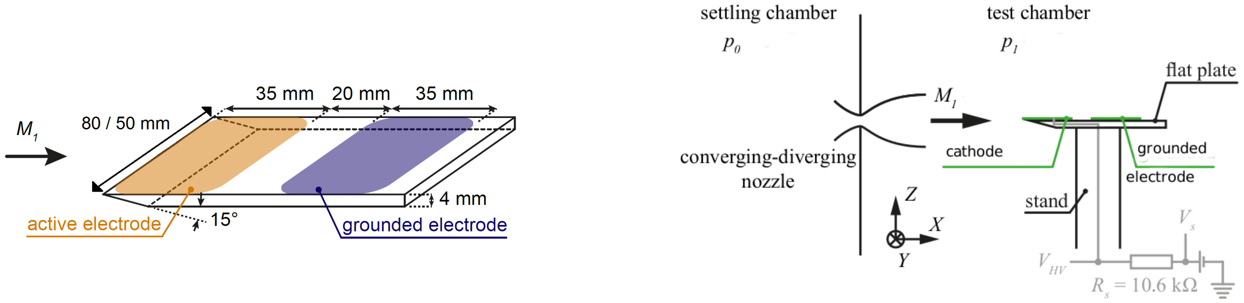

Figure 2: Scheme of the flat plate with the plasma actuator (left) and Experimental set-up (right).

conditions lead to a Reynolds number of 290 cm^{-1} and a Knudsen number of 6.57×10^{-3} calculated with a reference length of 10 cm, corresponding to the length of the flat plate and therefore, ranking the flow in the rarefied regime between the free molecular and the continuum regime. The table 1 summarized the experimental working conditions of the present work.

Table 1: Mach 20 Flow operating conditions

Stagnation conditions	Free stream conditions
$p_0 = 3.5\ bars$	$p_1 = 0.068\ Pa$
$T_0 = 1100\ K$	$T_1 = 13.6\ K$
$\rho_0 = 3.065\ kg.m^{-3}$	$\rho_1 = 1.73 \times 10^{-5}\ kg.m^{-3}$
	$\mu_1 = 4.197 \times 10^{-5}\ Pa.s$
	$U_1 = 1501.96\ m.s^{-1}$
	$M_1 = 20.2$
	$\lambda_1 = 0.657\ mm$
	$R_e = 290\ cm^{-1}$

2.2 Models and plasma actuator

The model under investigation is a flat plate (100 mm-long, 80 mm-wide and 4 mm-thick) with a sharp leading edge (15°), as shown on Figure 2. The model is made of quartz in order to withstand the high surface temperatures reached when using the plasma actuator. The flat plate is placed on a profile stand in the test section, downstream the nozzle exit as sketched on Figure 2. The plasma actuator is composed of two aluminium electrodes, 80 mm -wide and 35 mm-long, 80 μm-thick. These electrodes are flush mounted on the upper surface of the flat plate (see Fig.2). The cathode is biased with a High-Voltage Pulsed Generator (HVPG).This power supply is a nanosecond high voltage power supply (HVPG) delivering high voltage discharges with output pulse amplitudes up to 25 kV and pulse repetition rates ranged between 1 Hz and 10 kHz. With respect to DC power supply, the advantage of HVPG power supply is the efficient ionization due to high reduced electric field E/N during pulses and the discharge stability because of short pulses duration. Experiments were carried out for different pulse repetition rates and output amplitude. For some cases, pre-ionization was required. For these cases, the anode was biased with the DC supply used to pre-ionize the gas before switching on the HVPG. This pre-ionization was mostly needed for low amplitude voltage such as $-1\ kV$ which was insufficient to ionize the gas and for a pulse frequencies greater of 10 kHz, whatever the pulse voltage applied to the cathode. The operating conditions of the HVPG applied for plasma actuation are $-1\ kV$, $-5\ kV$, $-10\ kV and - 15\ kV$ in output pulse voltage with pulse repetition rates of 500 Hz, 1 kHz, 5 kHz and 10 kHz.

2.3 Diagnostics

The flow conditions are ensured by accurate measurements of the pressure in the test chamber (static pressure) and in the settling chamber (stagnation pressure). For this purpose, these pressures are measured with absolute capacitive sensors (MKS, 600 series Baratron); the scales are adapted to the range of the measured values. A set of manometers is available covering different pressure range values, connected to an MKS control unit (PR 4000B) with a 12-bit reso-

DOI: 10.13009/EUCASS2019-786

lution for the continuous acquisition of these parameters.

The modifications of the flowfield around the flat plate induced by the plasma actuator is visualized with a PI-MAX Gen-II iCCD camera (1024 × 1024-pixel array) equipped with a VUV objective lens (94 *mm*, $f/4.1$). The light is collected through a fluorine window located in the wall of the test section chamber. An intensified CCD camera (iCCD) is very efficient in our applications despite the low light conditions thanks to the presence of the CCD sensor and the image intensifier mounted in front of it. A CCD sensor is designed to convert an electromagnetic wave into a similar signal. When an image intensifier is added, the intensifier multiplies the incoming photons and supplies the CCD sensor with a large number of photons. A Pelletier cooler is connected to the camera to ensure low temperatures, thus minimizing the noise. The quality of the images obtained with the camera is regulated through a good balance between the exposure time and the intensifier gain rate.

The modifications of the surface plate temperature produced by the actuation of the plasma discharge is measured by Infrared thermography. The temperature distribution of the flat plate during experiments is obtained with an OPTRIS PI 400 camera. The spectral range of the IR camera lies between 7.5 μm and 13 μm. The IR camera was placed on top of the wind tunnel and focused the entire surface of the flat plate through a selenium zinc window (ZnSe), compatible with the IR wavelength range of the camera. The viewing angle remained unchanged throughout the experiments. The aperture of the lens used in this study was a O13 Telephoto lens $13° \times 10°$ (FOV) with an image resolution of 0.61 *mrad* (IFOV). The detector sensitivity covers a surface of 382 × 288 *pixels* for a thermal image recording in real time up to 80 *Hz*. The focus length between the flat plate surface and the IR camera was 1395 *mm* ± 10 *mm*, giving a spatial resolution of 0.84 $mm.pixel^{-1}$ ± 0.01 $mm.pixel^{-1}$ along both X and Y axes. Focusing of the IR camera was performed before each run of the wind tunnel by placing a heated coin (head side) on the flat plate surface. The IR camera focusing was adjusted until the head side of the coin could be distinguished as clearly as possible. Due to the wide range of temperatures of the model, three acquisition ranges of the IR camera were applied during experiments, depending on the maximum temperature reached at the actuator surface. The first temperature range was between $0°C$ and $250°C$, with an accuracy of $\pm5°C$. The second one was between $-20°C$ and $100°C$, with an accuracy of $\pm5°C$ and the third one between $20°C$ and $500°C$, with an accuracy of $\pm5°C$. The thermal sensitivity (NEDT), corresponding to the smallest temperature differences detectable by the IR camera, was less than $0.1\,K$ for the three ranges.

3. Results

3.1 Baseline

In view to analyse the shock wave modifications induced by the plasma actuator, the baseline flowfield around the sharp flat plate was first studied. Because of the low density obtained in the test chamber with the Mach 20.2 hypersonic nozzle, the usual visualization methods such as strioscopy or interferometry are ineffective. Thus, the luminescence technique was applied to can observe the interactions of the flowfield and the flat plate. The method consists in polarizing two metal plates placed on both sides of the nozzle above the plate in order to capture the whole shock wave. The light emit by this slightly glow discharge is captured by a series of 100 images with the iCCD camera that are post-processed using Matlab imaging toolbox. To highlight the shock wave, background images of the flow without the model are subtracted from images with the flat plate in view to increase the contrast. Figure 3 shows clearly the flat plate and the attached oblique shock wave for two angles of attack.

With no angle of attack, the baseline shock wave angle was determined from the average of five series of 100 images, giving $\beta = 15.2° \pm 0.5°$. Vertical intensity profiles are retrieved from Figure 3 for four X-positions along the plate at 25 *mm*, 35 *mm*, 50 *mm* and 75 *mm* and normalized to the free stream value in order to be compared. These positions are useful to follow the evolution of the shock wave on the surface of the flat plate and validate the value of the measured shock wave angle.

3.2 Flow field modification by the plasma actuator

Figure 5 presents the Mach 20 flow field around the flat plate modified by the plasma actuator with the pulsed discharge acting at 10 kHz and -1 kV. The new shock wave observed is is rounded close to the leading edge where the active electrode is placed. The ionized region is very wide, with a strong ionization in the region above the cathode as can be seen on the iCCD image, making the acquisition and the analysis of these images quite difficult. The plasma sheath is barely visible.

DOI: 10.13009/EUCASS2019-786

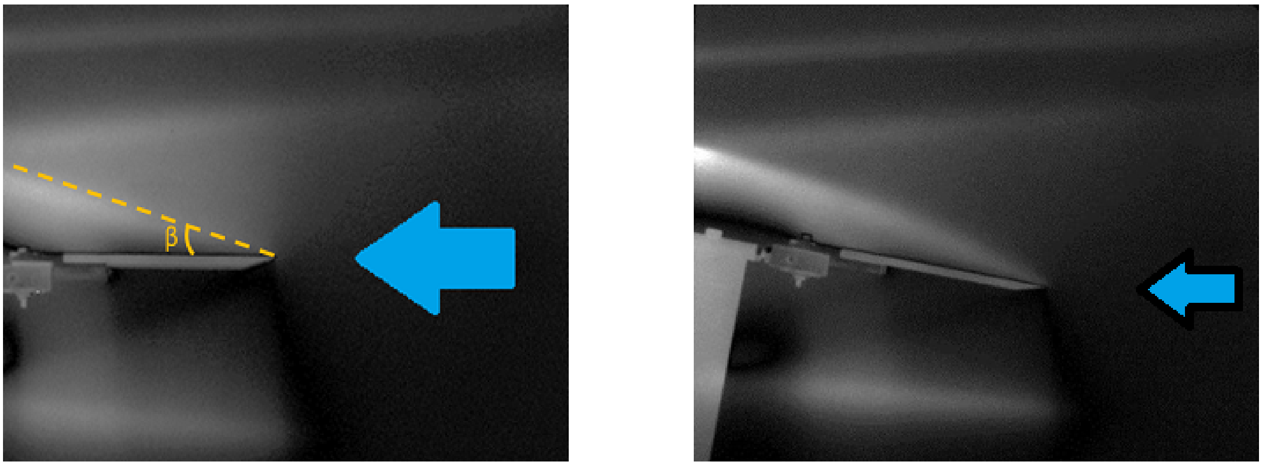

Figure 3: iCCD image of the flat plate in the Mach 20 flow with an angle of attack of 0°, *i.e.* the baseline (left) and with an angle of attack of −10°. (rigth)

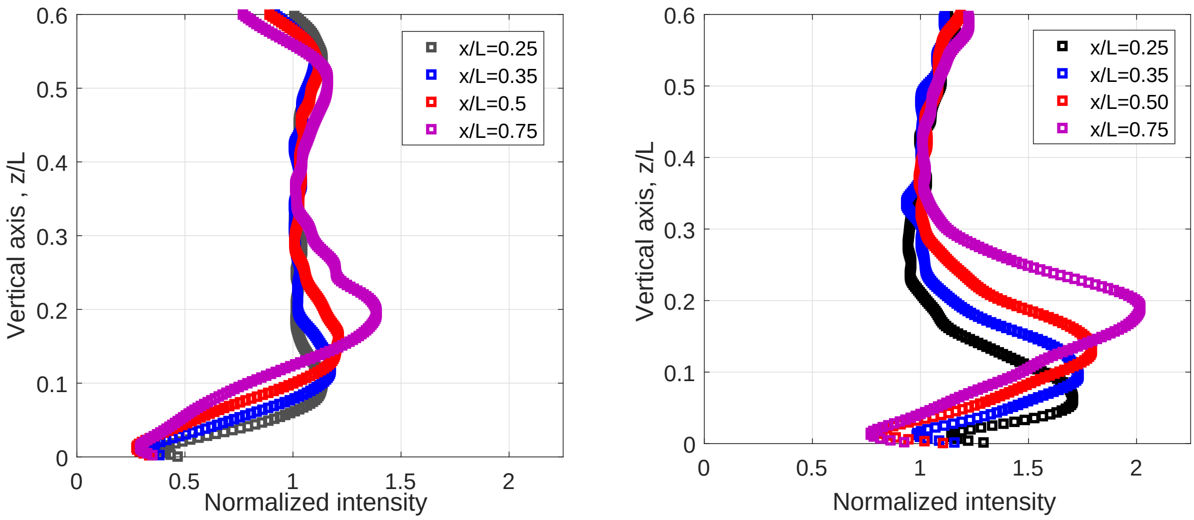

Figure 4: Experimental density profiles retrieved from the iCCD images for an angle of attack of 0° (left) and an angle of attack of −10° (right).

DOI: 10.13009/EUCASS2019-786

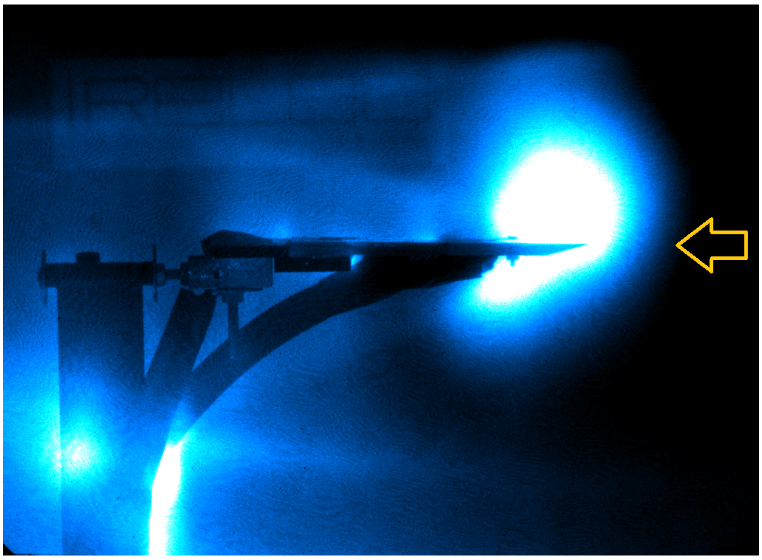

Figure 5: iCCD image of the pulsed discharge for 10 kHz and -1 kV in the hypersonic flow.

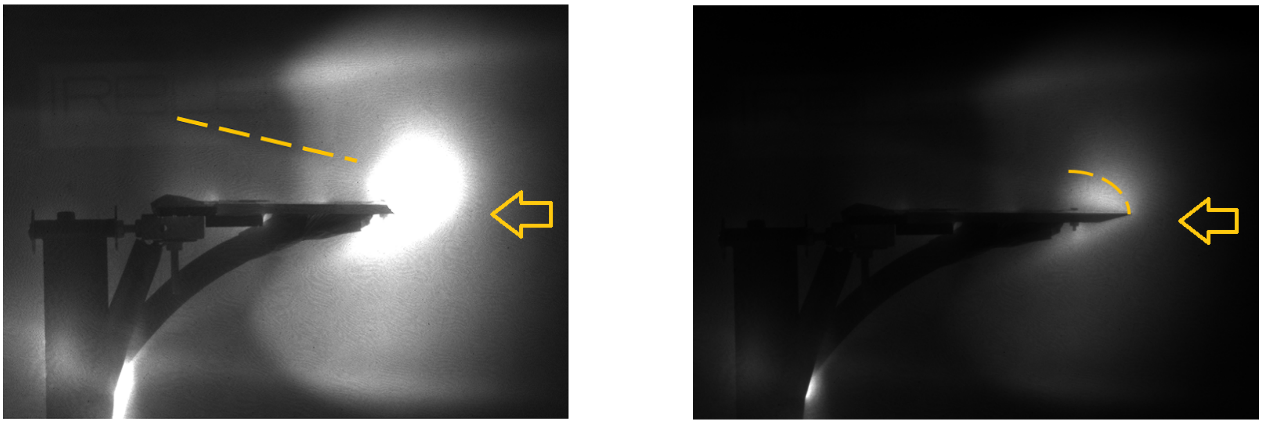

Figure 6: iCCD images of the flowfield modified with a discharge of -1 kV and 5 kHz, recorded with two different settings: (left) camera gain of 150 and camera gain of 110(right). The yellow dashed line represents the shock wave.

To better define the shock wave over the entire length of the plate, iCCD acquisitions were performed with two camera gains, the lower adjusted to the light emitted above the cathode and the greater adjusted to the emission of the wake. To illustrate this method, Figure 6, shows the image obtained for -1 kV and 5 kHz, on the left with a camera gain of 150 whereas on the right, the image was recorded with a camera gain of 110. Therefore, on the left, the contrast is enhanced on the back of the shock wave and on the right, the iCCD image is more contrasted close to the leading edge, making it possible to see the anchoring of the shock wave.

3.3 Surface thermal effects of the pulsed discharge

With hypersonic and rarefied regime, boundary layers above a flat plate are thick and merged with the shock wave,[2].[17] The thickness of the boundary layer is dependant on the surface plate temperature and an increase of the surface temperature leads to the thicken of the boundary layer. To assess the influence of the pulsed discharge on the surface temperature distribution along the flat plate, thermal Infra-Red measurements were carried out for every discharge configuration studied during experiments. Figure 7 plots the surface temperatures on the upper surface of the flat plate for the different repetition pulse rates and voltages applied to the active electrode. The frequencies are represented by the same types of lines: plain for 1 kHz, diamonds for 5 kHz, dots for 10 kHz, squares for 500 Hz. The voltages can be distinguished by color: violet for -1 kV, green for -5 kV, blue for -10 kV and yellow for -15 kV. The baseline is plotted with plain black line. The highest temperatures correspond to the 5 kHz case. The profile for the highest voltage, *i.e.* -15 kV, even exhibits temperatures two times higher than the other profiles. The temperature distributions for the

DOI: 10.13009/EUCASS2019-786

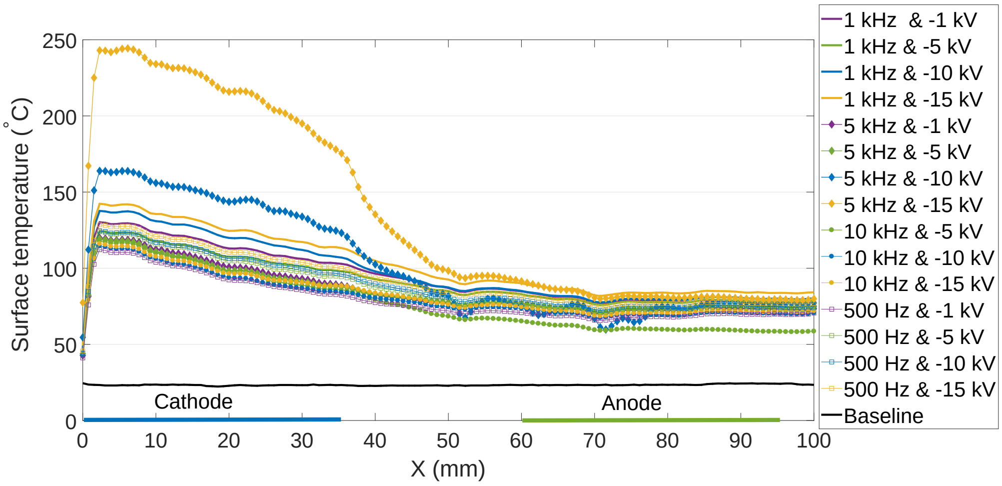

Figure 7: Surface temperatures on the upper surface of the flat plate for the different cases studied.

hypersonic flow presents a maximum value close to the leading edge and then a slightly decrease of the temperatures. The temperatures above the anode are constant, denoting the low impact of the discharge discharge. Moreover, the temperatures increase to more than $100°C$. The lower temperatures are still found for 500 Hz and the lowest voltage.

3.4 Shock wave shapes determination

The shock wave angle is hard to determine because of the rounded shape of the shock wave. Therefore, a program developed with Matlab is applied to detect and plot the shock shape for each test case from the processed iCCD images. The influence of the repetition rate pulse is plotted on Figure 8 where the voltage $-1\ kV$ is represented in magenta, $-5\,kV$ in green, $-10\,kV$ in blue and $-15\,kV$ in yellow. Symbols are used to highlight the cases where pre-ionization was applied to the anode in addition to the pulsed discharge, with dots for $V_{DC} = -200\ V$ and with triangles for $-500\ V$. Compared to the black broken line representing the baseline shock, all the experimental conditions modified the shock wave shape by pushing it upward. The shape is rounded above the cathode and this effect increases with the discharge voltage. This modification is more pronounced near the leading edge while at the end of the plate, the shape is closer to the baseline one. This behaviour was particularly observed for a frequency of 5 kHz. For discharges at 10 kHz, the shock detaches from the leading edge, mostly for high voltages. While the influence of the pre-ionization DC voltage applied at the anode was weak, nevertheless it seemed to prevent the shock from returning to the baseline shock as can be easily observed for 10 kHz and $-15\ kV$. The shock under the plate is also influenced by the discharge as the angle increases with the pulsed discharge voltage as presented on Figure 8 presenting the 10 kHz results.

Figure 9 plots the the shock wave shapes the different output pulse voltages studied to appreciate better their influence on the flow field modification. At first sight, for low voltages, the frequency does not account for much whereas there is an influence for the voltage $-1\ kV$ and $-10\ kV$. However, for $-10\ kV$, the rounded shape is enhanced for 1 kHz and 10 kHz. Visually, for all the frequencies, the shock wave expands in accordance with the increase in the voltage. Indeed, discharge voltages of $-15\ kV$ seem to have an effect as the shock wave is deviated a little more with respect to the baseline.

These results obtained with the pulsed discharge are reminiscent of those obtained without an actuator, when imposing an angle of attack on the plate. Figure 10 shows the comparison between shock wave shapes obtained with the pulsed discharge operating with a frequency of $5\,kHz$ and discharge voltages of -10 and $-15\,kV$ and the shock wave shapes obtained with an angle of attack of $-10°$ for the plate. As observed, the shock wave shapes perfectly agree in the region above the cathode particularly on the curve of the shock wave. Then the shock wave shape obtained with the actuator returns to the baseline shock profile whereas the shock wave obtained with the inclined plate remains lifted.

This result shows that in these flow regime conditions, the plasma actuator biased with a pulsed discharge may be able to modify the shock wave shape in a similar way as induced by an angle of attack and thus, probably also lead to an increase in the drag over a flat plate. Figure 10 shows the best fit among the different pulsed discharge configurations. Therefore, this effect could be adjusted by modulating the discharge voltage and frequency and even changing the actuator size, with with the aim of extending the region of actuation.

DOI: 10.13009/EUCASS2019-786

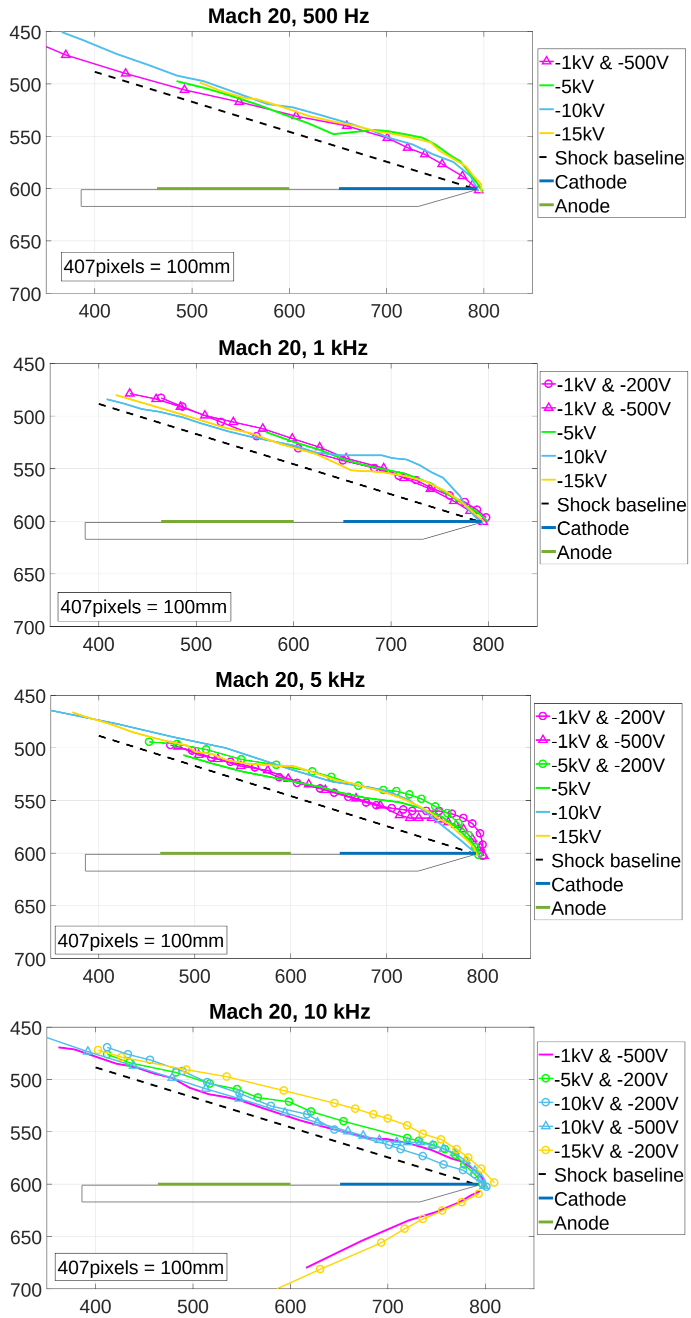

Figure 8: Shock wave shapes determined for different applied output pulse voltages: 500 Hz, 1 kHz, 5 kHz and 10 kHz.

DOI: 10.13009/EUCASS2019-786

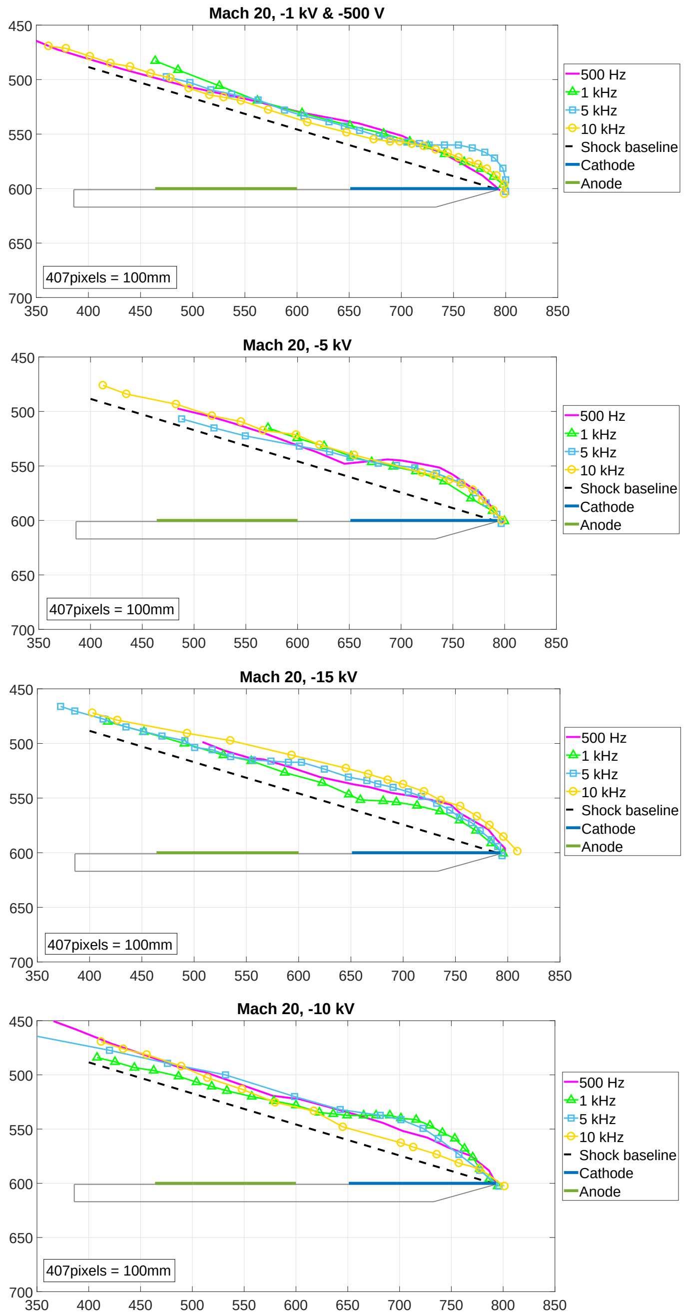

Figure 9: Shock wave shapes for different repetition rate pulse: $-1\ kV$, $-5\ kV$, $-10\ kV$ and $-15\ kV$.

DOI: 10.13009/EUCASS2019-786

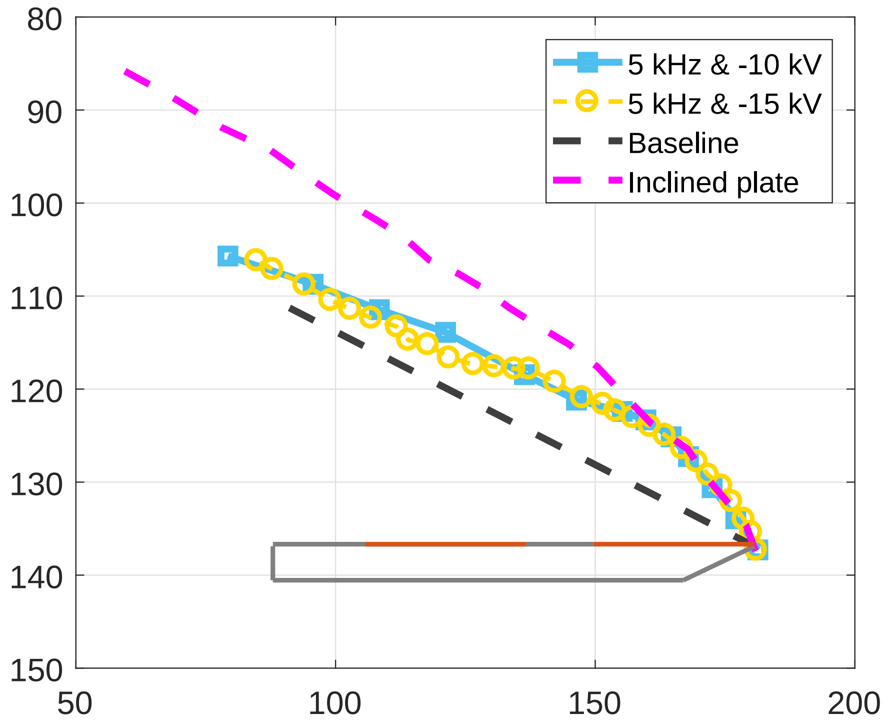

Figure 10: Comparison of the shock wave shapes obtained with pulsed plasma actuator (5 kHz and -10 and -15 kV) and with the flat plate at $-10°$ angle of attack.

4. Conclusions

This preliminary work presents an experimental study showing the ability of plasma actuators to modify shock waves above a flat plate in hypersonic and rarefied regime. Experiments were carried out with the facility Marhy with a Mach 20.2 flow and an ambient pressure simulating 100 km in altitude.A nanosecond pulsed power supply was used to supply the plasma actuator because gas ionisation is more efficient than a DC power supply at the low working pressure. An effect on the shock wave shape was clearly observed, mostly above the active cathode where the shock shape is rounded. This induces the increase of the shock wave angle for every experimented plasma actuator configuration. This results can be compared to those obtained with truncated plates or sharp plates with attack angles, where the shock wave angle are increased inducing an increase on drag forces applied to the plate. Future diagnostic developments such a two components balance will allow to measure a validate the efficiency of plasma actuators on the aerodynamic behaviour over the sharp flat plate.

5. Acknowledgments

This work was supported by the French Governement's Investissement d'Avenir program: Laboratoire d'Exellence CAPRYSSES (Grant NÂ° ANR-11-LABX-0006-01).

References

[1] J Allegre. The sr3 low density wind tunnel. facility capabilities and research development. In *28th Joint Propulsion Conference and Exhibit*, page 3972, 1992.

[2] Jean Allegre, Michel Raffin, Amer Chpoun, and Louis Gottesdiener. Rarefied hypersonic flow over a flat plate with truncated leading edge. *Progress in Astronautics and Aeronautics*, 160:285–285, 1994.

[3] Sandra Coumar. *Study of physical mechanisms induced by a plasma actuator for super/hypersonic rarefied flows applied to atmospheric entries.* PhD thesis, Université d'Orléans, 2017.

DOI: 10.13009/EUCASS2019-786

[4] Sandra Coumar, Romain Joussot, Jean-Denis Parisse, and Viviana Lago. Effect of surface heating on shock wave modification by a plasma actuator in a rarefied supersonic flow over a flat plate. In *20th AIAA International Space Planes and Hypersonic Systems and Technologies Conference*, page 3562, 2015.

[5] Sandra Coumar, Romain Joussot, Jean Denis Parisse, and Viviana Lago. Influence of a plasma actuator on aerodynamic forces over a flat plate interacting with a rarefied mach 2 flow. *International Journal of Numerical Methods for Heat & Fluid Flow*, 26(7):2081–2100, 2016.

[6] Sandra Coumar and Viviana Lago. Influence of mach number and static pressure on plasma flow control of supersonic and rarefied flows around a sharp flat plate. *Experiments in Fluids*, 58(6):74, 2017.

[7] Patrick Gallais. *Atmospheric re-entry vehicle mechanics*. Springer Science & Business Media, 2007.

[8] Romain Joussot and Viviana Lago. Experimental investigation of the properties of a glow discharge used as plasma actuator applied to rarefied supersonic flow control around a flat plate. *IEEE Transactions on Dielectrics and Electrical Insulation*, 23(2):671–682, 2016.

[9] Romain Joussot, Viviana Lago, and Jean-Denis Parisse. Quantification of the effect of surface heating on shock wave modification by a plasma actuator in a low-density supersonic flow over a flat plate. *Experiments in Fluids*, 56(5):1–18, 2015.

[10] Konstantinos Kourtzanidis, Laxminarayan L Raja, Sandra Coumar, and Viviana Lago. Numerical simulation of dc glow discharges for shock wave modification. In *54th AIAA Aerospace Sciences Meeting*, page 2157, 2016.

[11] V Lago, Romain Joussot, and JD Parisse. Influence of the ionization rate of a plasma discharge applied to the modification of a supersonic low reynolds number flow field around a cylinder. *Journal of Physics D: Applied Physics*, 47(12):125202, 2014.

[12] V Lago, JC Lengrand, E Menier, TG Elizarova, AA Khokhlov, and T Abe. Physical interpretation of the influence of a dc discharge on a supersonic rarefied flow over a flat plate. In *Aip Conference Proceedings*, volume 1084, page 901, 2008.

[13] Wiley J Larson and Jerry Jon Sellers. *Understanding space: an introduction to astronautics*. McGraw-Hill, 1994.

[14] E Menier, L Leger, E Depussay, V Lago, and G Artana. Effect of a dc discharge on the supersonic rarefied air flow over a flat plate. , 40(3):695–701, 2007.

[15] Eric Menier. *Influence d'une décharge électrique continue sur un écoulement supersonique raréfié*. PhD thesis, Orléans, 2007.

[16] Peter Palm, Rodney Meyer, Elke Pl-ograve, njes, J William Rich, and Igor V Adamovich. Nonequilibrium radio frequency discharge plasma effect on conical shock wave: M= 2.5 flow. *AIAA journal*, 41(3):465–469, 2003.

[17] M Raffin. Rarefied hypersonic flow over a sharp flat plate: numerical and experimental results. In *Rarefied Gas Dynamics: Technical Papers from the Proceedings of the Eighteenth International Symposium on Rarefied Gas Dynamics, University of British Columbia, Vancouver, British Columbia, Canada, July 26-30, 1992...*, volume 160, page 276. American Institute of Aeronautics and Astronautics, Incorporated, 1994.

[18] J Shin, V Narayanaswamy, L Raja, and N T Clemens. Characteristics of a plasma actuator in mach 3 flow. In *AIAA Paper No. 2007–788*, 2007.

[19] Sergey T Surzhikov and Joseph S Shang. Two-component plasma model for two-dimensional glow discharge in magnetic field. *Journal of Computational Physics*, 199(2):437–464, 2004.